CrossMark

ORIGINAL PAPER

Pcal_1127, a highly stable and efficient ribose-5-phosphate pyrophosphokinase from *Pyrobaculum calidifontis*

Tahira Bibi[1] · Sumera Perveen[1] · Iram Aziz[1] · Qamar Bashir[1] · Naeem Rashid[1] ·
Tadayuki Imanaka[2] · Muhammad Akhtar[1,3]

Abstract Analysis of the genome sequence of *Pyrobaculum calidifontis* revealed the presence of an open reading frame Pcal_1127 annotated as ribose-5-phosphate pyrophosphokinase. To examine the properties of Pcal_1127 the coding gene was cloned, expressed in *Escherichia coli,* and the purified gene product was characterized. Pcal_1127 exhibited higher activity when ATP was replaced by dATP as pyrophosphate donor. Phosphate and EDTA activated the enzyme activity and equivalent amount of activity was detected with ATP and dATP in their presence. Recombinant Pcal_1127 could utilize all the four nucleotides as pyrophosphate donors with a marked preference for ATP. Optimum temperature and pH for the enzyme activity were 55 °C and 10.5, respectively. A unique feature of Pcal_1127 was its stability against temperature as well as denaturants. Pcal_1127 exhibited more than 95 % residual activity after heating for 4 h at 90 °C and a half-life of 15 min in the boiling water. The enzyme activity was not affected by the presence of 8 M urea or 4 M guanidinium chloride. Pcal_1127 was a highly efficient enzyme with a catalytic efficiency of 5183 mM^{-1} s^{-1}. These features make Pcal_1127, a novel and unique ribose-5-phosphate pyrophosphokinase.

Communicated by H. Atomi.

✉ Naeem Rashid
naeemrashid37@hotmail.com; naeem.ff.sbs@pu.edu.pk

1   School of Biological Sciences, University of the Punjab, Quaid-e-Azam Campus, Lahore 54590, Pakistan

2   The Research Organization of Science and Technology, Ritsumeikan University, Kusatsu, Shiga 525-8577, Japan

3   School of Biological Sciences, University of Southampton, Southampton SO16 7PX, UK

Introduction

Ribose-5-phosphate pyrophosphokinase (RPPK, EC 2.7.6.1) catalyzes the transfer of pyrophosphoryl group from ATP to C1 hydroxyl group of ribose-5-phosphate resulting in the production of phosphoribosyl pyrophosphate (PRPP) and AMP. PRPP plays a central role in several processes of life, including the synthesis of nucleotides, co-enzyme NAD$^+$, and amino acids histidine and tryptophan (Hove-Jensen 1988). RPPK has been characterized from all the three domains of life, including eukarya, bacteria, and archaea. Among eukaryotes, it has been studied from *Saccharomyces cerevisiae* (Hove-Jensen 2004), *Ashbya gosypii* (Jiménez et al. 2008), *Arabidopsis thaliana* (Krath et al. 1999), spinach (Krath and Hove-Jensen 2001a), mosquito (Hong et al. 2013), rat (Roth et al. 1974, Kita et al. 1989), and human (Nosal et al. 1993). The bacteria from which RPPK has been investigated include *Salmonella typhimurium* (Switzer 1969), *Escherichia coli* (Willemoës et al. 2000), *Bacillus subtilis* (Arnvig et al. 1990), *Bacillus amyloliquefaciens* (Zakataeva et al. 2012), and *Mycobacterium tuberculosis* (Lucarelli et al. 2010). Among archaea, the third domain of life, it has been characterized from *Thermococcus kodakarensis* (Rashid et al. 1997), *Methanocaldococcus jannaschii* (Kadziola et al. 2005), *Thermoplasma volcanium* (Cherney et al. 2011), and *Sulfolobus solfataricus* (Andersen et al. 2015).

Based upon their properties, RPPKs can be divided into three classes. Class I enzymes are limited to ATP and, in some cases, dATP in their specificity for pyrophosphoryl

donors. They are allosterically inhibited either by ADP or GDP or both. Furthermore, they are activated by phosphate, which may be regarded as an allosteric activator as phosphate binding competes with ribonucleoside diphosphate binding at the allosteric site (Willemoës et al. 2000). Class II shows broad pyrophosphoryl donor specificity by accepting GTP, CTP, or UTP (in addition to ATP and dATP). Allosteric regulation has not been detected in this class and their activity is independent of phosphate (Krath and Hove-Jensen 2001a, b). Members of class III do not appear to be allosterically regulated by ribonucleoside diphosphate, but activated by phosphate (Kadziola et al. 2005). Thus, the characteristics of this class are a mixture of those of class I and II.

Here, we report cloning and characterization of an efficient RPPK from the hyperthermophilic archaeon *Pyrobaculum calidifontis,* a facultative aerobe that grows optimally between 90 and 95 °C (Amo et al. 2002). The complete genome of the microorganism has been determined (http://www.ncbi.nlm.nih.gov/nuccore/CP000561.1). Genome search revealed the presence of an open reading frame Pcal_1127 annotated as ribose-5-phosphate pyrophosphokinase. To get functional information, we expressed the gene encoding Pcal_1127 in *E. coli* and characterized the gene product.

Materials and methods

Chemicals and materials were purchased either from Sigma Aldrich Co. or Thermo-Fisher Scientific Inc. or Fluka Chemical Corp. Cloning vectors, restriction enzymes and DNA purification kits were purchased from Thermo-Fisher Scientific Inc. Gene-specific oligonucleotides were commercially synthesized from Macrogen Inc. Vectors, pTZ57R/T (Thermo-Fisher), and pET-21a (Novagen, Madison, WI, USA) were employed for cloning and expression purposes, respectively. *E. coli* cells DH5α and BL21-CodonPlus(DE3)-RIL (Stratagene, La Jolla, CA, USA) were used for cloning and expression purposes.

Gene cloning, expression in *E. coli,* and purification of recombinant Pcal_1127

RPPK gene, Pcal_1127, from *P. calidifontis* was amplified by polymerase chain reaction (PCR) using sequence-specific forward, Pcal_1127F (5′ <u>CATATG</u>GACAAAATAAATAGCCGTGCTTTGTATACGCC 3′), and reverse, Pcal_1127R (5′ CTATAGCAGTTTCTC-CACCTCTC 3′), primers and genomic DNA of *P. calidifontis* as template. Recognition site for restriction enzyme *Nde*I (underlined sequence) was introduced in the forward primer. The PCR-amplified DNA fragment was ligated in cloning vector pTZ57R/T using T4 DNA ligase as recommended by the supplier (Thermo-Fisher Scientific Inc).

The resulting plasmid was named as pTZ_1127. Pcal_1127 gene was liberated from pTZ_1127 using *Nde*I (introduced in the forward primer) and *Hind* III (from multiple cloning sites of pTZ57R/T) restriction enzymes and cloned in pET-21a expression vector utilizing the same sites. The resulting recombinant plasmid was named as pET_1127.

Escherichia coli BL21-CodonPlus(DE3)-RIL were transformed using pET_1127. The transformed cells were cultivated in Luria–Bertani (LB) medium supplemented with 100 µg/mL ampicillin at 37 °C till an optical density of 0.4–0.5 at 660 nm was reached. The expression of the gene was induced by the addition of isopropyl-β-D-1-thiogalactopyranoside (IPTG) at a final concentration of 0.2 mM. After induction, the cells were allowed to grow for 4–6 h at 37 °C and harvested by centrifugation. Cell pellet (3 g wet weight from 1 L culture) was resuspended in 30 mL of 50 mM Tris–Cl buffer of pH 8 containing 0.2 mM phenylmethylsulfonyl fluoride and β-mercaptoethanol. Cells were then lysed by sonication. Soluble and insoluble fractions were separated and supernatant containing recombinant Pcal_1127 was heated at 80 °C for 25 min to denature the heat-labile proteins of *E. coli*. The denatured proteins were removed by centrifugation at $20,000 \times g$ for 20 min. The supernatant containing Pcal_1127 was loaded onto HiTrap Q anion exchange column.

The proteins were eluted using a linear gradient of 0–1 M NaCl. The fractions having the desired protein were pooled, dialyzed, and loaded onto Resource Q anion exchange column. The proteins were eluted in a similar way as described above. Protein concentration was determined spectrophotometrically at every step of purification using Bradford reagent (Bradford 1976).

Molecular mass determination

The molecular mass of recombinant Pcal_1127 was determined by the SDS-PAGE analysis as well by gel filtration chromatography. For gel filtration chromatography, Superdex 200 10/300 GL gel filtration column (GE Healthcare) was equilibrated with 150 mM NaCl in 20 mM Tris–Cl (pH 8). The standard curve was obtained with ferritin (440 kDa), catalase (240 kDa), lactate dehydrogenase (140 kDa), BSA (64.5 kDa), and proteinase K (28.9 kDa). Solutions of the standard and sample proteins were prepared in 20 mM Tris–Cl (pH 8) containing 150 mM NaCl.

Enzyme assay

Enzyme activity of Pcal_1127 was measured by flourometric coupling reaction. Formation of PRPP from ribose 5-phosphate (R-5P) was measured through its utilization by anthranilate phosphoribosyl transferase (TrpD) to form *N*-5′-phosphoribosyl anthranilate (PRA) as summarized

below. The absorption and emission wavelengths for anthranilic acid (AA) are 315 and 390 nm, respectively. Anthranilic acid reacted with PRPP (produced by Pcal_1127) and its utilization resulted in decrease in emission/fluorescence at 390 nm.

$$R\text{-}5P + ATP \rightarrow PRPP + AMP$$

$$PRPP + AA \leftrightarrow PRA + PPi.$$
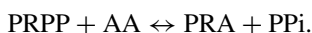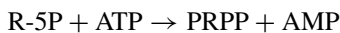
Assay mixture contained 1 mM R-5P, 5 mM MgCl$_2$, 2.5 mM ATP, 100 mM Tris–Cl buffer pH 8.5, 25 μM anthranilic acid, 100 μM ZnCl$_2$, 20 μg BSA, 1 mM EDTA, 20 μg of RPPK, and 100 μg of anthranilate phosphoribosyl transferase in a total volume of 2 mL. For estimation of optimal temperature for Pcal_1127, enzyme assays were performed at various temperatures ranging from 40 to 80 °C keeping the pH constant. For estimation of optimal pH, assays were performed at various pH keeping the temperature at 55 °C.

One unit of enzyme activity is defined as the amount of enzyme required to catalyze the synthesis of 1 μmol of PRPP per min which is equivalent to disappearance of 1 μmol of anthranilic acid per min.

For thermostability experiments, Pcal_1127, in 20 mM Tris–HCl, was heated at 90 °C for various intervals of time and the residual activity was examined at 55 °C and pH 10.5 in 50 mM glycine-NaOH buffer.

Circular dichroism analysis

Structural stability of Pcal_1127 was analyzed by circular dichroism (CD) spectroscopy using Chirascan-plus CD Spectrometer (Applied Photophysics, UK). The protein samples were incubated at different temperatures ranging from 50 to 100 °C. The CD spectra of the protein solutions were recorded in 20 mM Tris–Cl pH 8.0 in the far-UV range of 200–260 nm. Solvent spectra were subtracted from those of the protein solutions.

Denaturation studies of Pcal_1127

For denaturation studies, protein samples were prepared in different concentrations of urea (0–8 M final concentration) or guanidinium chloride (0–6 M final concentration) and incubated at room temperature for 30 min. Residual enzyme activity of these samples was examined as described above.

Results

Genome search of *P. calidifontis* revealed the presence of an open reading frame, Pcal_1127, annotated as ribose-5-phosphate pyrophosphokinase. The gene consisted of 891 nucleotides encoding a polypeptide of 297 amino acids having a theoretical molecular mass of 32,741 Da and an isoelectric point of 6.97. Pcal_1127 displayed highest identity of 76 % with an uncharacterized enzyme from *Pyrobaculum neutrophilum*. Among the characterized enzymes, Pcal_1127 displayed highest identity of 38 % with RPPK from *T. kodakarensis* and *S. solfataricus*. When amino acid sequences of the characterized members of this family were aligned and a phylogenetic tree was constructed, three distinct groups were demarcated. Group I consists of RPPKs from eukarya and bacteria, including *S. cerevisiae*, human, rat, spinach, *A. thaliana*, *B. subtilis*, *M. tuberculosis*, *S. typhimurium*, *E. coli*, and *B. amyloliquefaciens*. Group II seems to be specific for plants. It comprises two isozymes from spinach and two from *A. thaliana*. Pcal_1127, along with all the RPPKs characterized from archaea, neither cluster in group I nor in group II. Archaeal RPPKs make a third and relatively dispersed group (Fig. 1). Alignment of amino-acid sequences of all the characterized RPPKs revealed the presence of six highly conserved regions. Regions I to IV contain active-site residues (typed bold in Fig. 2) according to the crystal structures of RPPK from *B. subtilis*, *M. jannaschii,* and *S. solfataricus*. They are involved in substrate binding. In these regions, [41]Phe, [43]Asp and [45]Glu (Region I), [102]Arg and [103]Gln (Region II), [134]Asp and [136]His (Region III), and [198]Lys and [200]Arg (Region IV), according to *B. subtilis* numbering, are involved in ATP binding. [41]Phe, [43]Asp, and [45]Glu define specificity for adenine base. [198]Lys and [200]Arg are involved in the binding of triphosphate chain of ATP and stabilization of transition state (Eriksen et al. 2000; Kadziola et al. 2005; Andersen et al. 2015). All these residues are conserved in Pcal_1127. Region V is reported to be involved in substrate (R-5P) binding in the enzymes from above three microorganisms. This region is highly conserved in archaea. In this region, amino-acid residues [224]Asp, [225]Asp, [231]Gly, and [232]Thr are conserved in all the characterized RPPKs. Region VI has been reported to play a role in allosteric regulation in RPPKs from *B. subtilis* and human (Eriksen et al. 2000; Li et al. 2007). This region is found only in class I RPPKs which are allosterically regulated and absent in the characterized members of class II and III (Fig. 2). These results are consistent with the experimental data demonstrating that class II and III enzymes are not allosterically regulated (Krath and Hove-Jensen 2001a; Kadziola et al. 2005).

Production and purification of recombinant Pcal_1127

Analysis of production of recombinant Pcal_1127 in *E. coli* cells harboring pET-1127, by SDS-PAGE, demonstrated that a high amount of Pcal_1127 was produced in
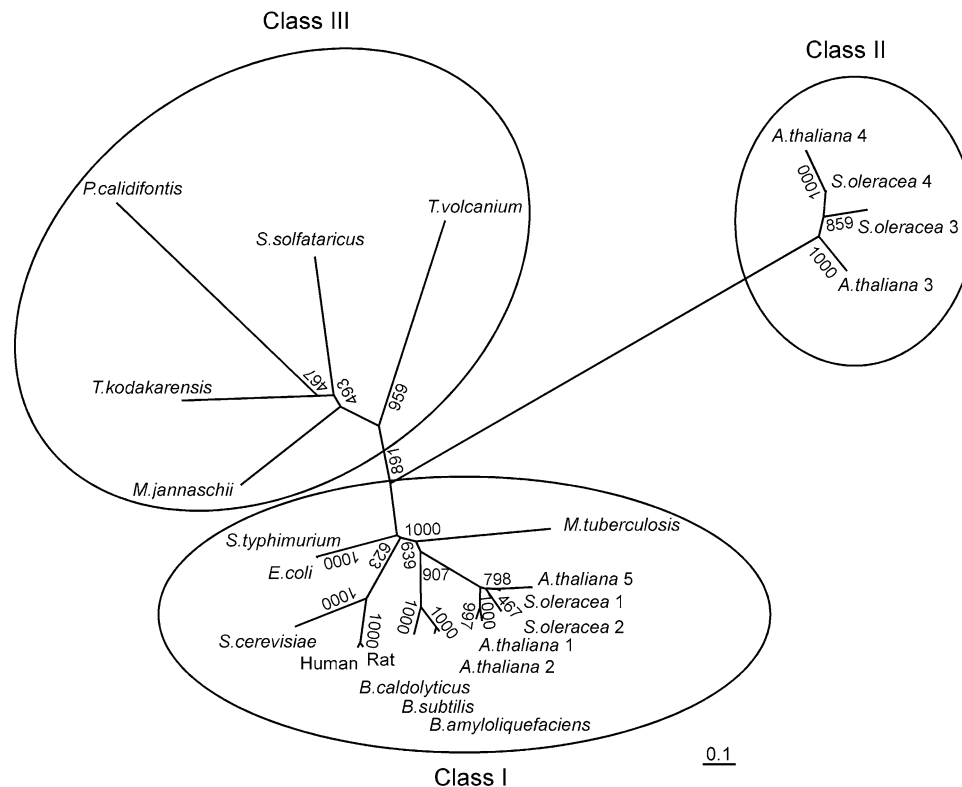
Fig. 1 Phylogenetic tree of Pcal_1127 and all the characterized RPPKs, whose amino-acid sequences are available in the database. Unrooted tree with branch length was constructed using the neighbor-joining method. Bootstrap values and segments corresponding to an evolutionary distance of 0.1 are shown. The tree was constructed using ClustalW provided at http://clustalw.ddbj.nig.ac.jp/. Following are the sequences, with accession numbers, used for the alignment to construct the phylogenetic tree: *P. calidifontis* (Pcal_1127), ABO08552; *S. solfataricus*, AAK41307; *T. kodakarensis*, BAD86424; *M. jannaschii*, AAB99374; *T. volcanium*, Q97CA5; *B. subtilis*, P14193; *B. amyloliquefaciens*, CBI41177; *B. caldolyticus*, P42816; *S. typhimurium*, P0A1V6; *E. coli*, P0A717; *M. tuberculosis*, P9WKE3; *S. cerevisiae*, P38063; Human, P60891; rat, P09330; *A. thaliana*, Q42581, Q42583, Q93Z66, Q680A5, Q64888; and *S. oleracea*, Q9XG98, Q9XG99, Q9XGA0, Q9XGA1

the cells induced with IPTG. Recombinant Pcal_1127 was more than 20 % of the total proteins of the host. When the soluble and insoluble fractions, after lysis, were analyzed, it was found that recombinant Pcal_1127 was produced in the soluble form (Fig. 3). The first step of purification was based on the thermostability of recombinant Pcal_1127. The protein sample was heated at 80 °C which resulted in precipitation and removal of most of the heat-labile proteins of the host. Further purification by ion exchange column chromatography using HiTrap Q and Resource Q columns resulted in a final yield of 17 % with a 4.6-fold-purification (Table 1).

Molecular mass determination

Molecular mass and subunit number of recombinant Pcal_1127 were determined by gel filtration chromatography. Pcal_1127 eluted at a retention volume of 15.8 mL, which corresponded to an approximate molecular mass of 32 kDa on a standard curve obtained from the elution volumes of various standard proteins of known molecular weight (data not shown). This indicated that the recombinant Pcal_1127 existed in a monomeric form similar to RPPK from *T. kodakarensis* (Rashid et al. 1997). All other RPPKs, characterized either from bacteria, eukarya, or archaea, exist in more than one identical subunits (Roth et al. 1974; Kadziola et al. 2005; Cherney et al. 2011; Andersen et al. 2015; Li et al. 2007; Hove-Jensen and McGuire 2004).

Biochemical characterization of Pcal_1127

The enzyme activity of Pcal_1127 was examined in Britton–Robinson buffer, a universal buffer, at various pH. The optimum pH for Pcal_1127 enzyme activity was 10.5. Activity decreased rapidly at pH above 10.5 (Fig. 4a). Pcal_1127 is the only RPPK that exhibits optimum activity at such a high pH.

When we examined the activity of Pcal_1127 at various temperatures, we found that the enzyme exhibited

Source	Region I	Region II	Region III	Region IV	Region V	Region VI	
B.subtilis	^{41}**F**SD**GE**	^{102}**RQD**R	^{134}**DLH**	^{198}**KRR**	^{224}**DD**IIDTA**GT**	^{311}**S**VSYL**F**	Class I
B.amyloliquefaciens	^{41}**F**SD**GE**	^{102}**RQD**R	^{134}**DLH**	^{198}**KRR**	^{224}**DD**IIDTA**GT**	^{311}**S**VSYL**F**	
B.caldolyticus	^{39}**F**SD**GE**	^{100}**RQD**R	^{132}**DLH**	^{196}**KRR**	^{222}**DD**IIDTA**GT**	^{309}**S**VSYL**F**	
H.sapiens	^{35}**F**SNQ**E**	^{96}**RQD**K	^{128}**DLH**	^{194}**KER**	^{220}**DD**MADTC**GT**	^{308}**S**VSYL**F**	
R.norvegicus	^{35}**F**SNQ**E**	^{96}**RQD**K	^{128}**DLH**	^{194}**KER**	^{220}**DD**MADTC**GT**	^{308}**S**VSYL**F**	
S.oleracea.1	^{57}**F**AD**GE**	^{118}**RAD**R	^{150}**DLH**	^{217}**KRR**	^{243}**DD**MIDTA**GT**	^{330}**S**VSSI**F**	
S.oleracea.2	^{115}**F**AD**GE**	^{177}**RAD**R	^{209}**DLH**	^{276}**KRR**	^{302}**DD**MIDTA**GT**	^{389}**S**VSSI**F**	
A.thaliana.1	^{124}**F**AD**GE**	^{185}**RAD**R	^{217}**DLH**	^{284}**KRR**	^{310}**DD**MIDTA**GT**	^{397}**S**VSSI**F**	
A.thaliana.2	^{121}**F**AD**GE**	^{182}**RAD**R	^{214}**DLH**	^{281}**KRR**	^{307}**DD**IIDTA**GT**	^{394}**S**VSSI**F**	
A.thaliana.5	^{109}**F**AD**GE**	^{170}**RAD**R	^{202}**DLH**	^{269}**KRR**	^{295}**DD**MIDTA**GT**	^{382}**S**GAIEP	
M.tuberculosis	^{43}**F**AN**GE**	^{104}**RQD**K	^{136}**DLH**	^{202}**KTR**	^{230}**DD**MIDTG**GT**	^{317}**S**VTGL**F**	
E.coli	^{34}**F**SD**GE**	^{96}**RQD**R	^{129}**DLH**	^{194}**KRR**	^{220}**DD**MIDTG**GT**	^{308}**S**ISAM**F**	
S.cerevisiae	^{45}**Y**SNK**E**	^{108}**RQD**K	^{140}**DLH**	^{205}**KER**	^{231}**DD**MADTC**GT**	^{316}**S**VSYL**F**	
S.typhimurium	^{35}**F**SD**GE**	^{96}**RQD**R	^{128}**DLH**	^{194}**KRR**	^{220}**DD**MIDTG**GT**	^{308}**S**ISAM**F**	
A.thaliana.3	^{133}**F**DD**GF**	^{194}**TSE**R	^{231}**DIH**	^{296}**KVR**	^{321}**DD**LVQSG**GT**	----------	Class II
A.thaliana.4	^{60}**F**AD**GF**	^{121}**SFE**R	^{158}**DIH**	^{223}**KVR**	^{248}**DD**LVQSG**GT**	----------	
S.oleracea.3	^{128}**F**ED**GF**	^{189}**TSE**R	^{226}**DIH**	^{291}**KVR**	^{316}**DD**LVQSG**GT**	----------	
S.oleracea.4	^{41}**F**DD**GF**	^{102}**SFE**R	^{139}**DIH**	^{204}**KVR**	^{229}**DD**LVQSG**GT**	----------	
M.jannaschii	^{39}**F**PD**GE**	^{99}**RQD**K	^{130}**NPH**	^{193}**KTR**	^{219}**DD**IISTG**GT**	----------	Class III
T.volcanium	^{32}**F**PD**GE**	^{91}**RQ**HQ	^{122}**DIH**	^{184}**KKR**	^{210}**DD**IISTG**GT**	----------	
S.solfataricus	^{35}**F**PD**GE**	^{96}**RQD**R	^{128}**EPH**	^{191}**KER**	^{219}**DD**IISTG**GT**	----------	
T.kodakarensis	^{30}**F**PD**GE**	^{89}**RQD**R	^{120}**DTH**	^{183}**KRR**	^{209}**DD**IISTG**GT**	----------	
P.calidifontis	^{42}**F**PD**GE**	^{101}**RQD**R	^{133}**DLH**	^{194}**KYR**	^{222}**DD**ILSTG**GT**	----------	

Fig. 2 Alignment of six conserved regions found in the characterized RPPKs. Regions I to IV contain the amino-acid residues of the active site of *M. jannaschii* (Kadziola et al. 2005) and *B. subtilis* (Eriksen et al. 2000). Region V is involved in the ribose 5-phosphate binding. Region VI has been reported to play a role in allosteric regulation which is present only in Class I RPPKs. Names at the *left hand side* indicate the source organism from which the sequence originated. The *numbers* show the position of the amino acid in the protein sequence
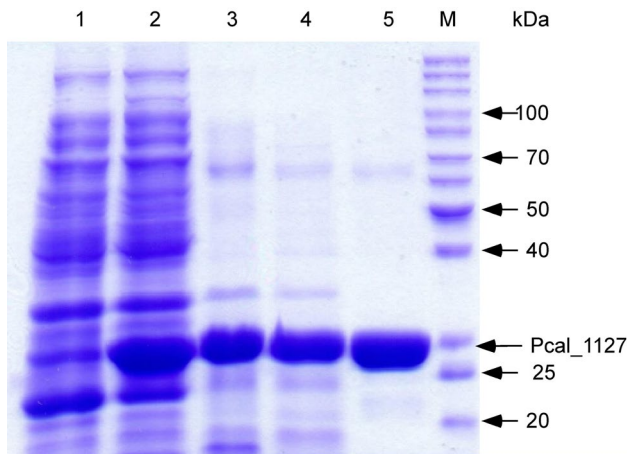

Fig. 3 Coomassie brilliant blue stained SDS-PAGE showing the purified recombinant Pcal_1127. Lane *1*, soluble fraction of *E. coli* cells harboring pET-21a; lane *2*, soluble fraction of *E. coli* cells containing pET-1127 plasmid; lane *3*, soluble fraction after heat treatment of sample from lane *2*; lane *4*, Pcal_1127 after HiTrap Q column; lane *5*, recombinant Pcal_1127 after Resource Q column; lane *M*, molecular mass marker

highest activity at 55 °C (Fig. 4b), although the optimal growth temperature of *P. calidifontis* is between 90 and 95 °C. This characteristic of Pcal_1127 is similar to other RPPKs from hyperthermophilic sources, including *T. kodakarensis* [50 °C; (Rashid et al. 1997)] and *S. solfataricus* [60 °C; (Andersen et al. 2015)]. RPPK from *M. jannaschii* is an exception which displayed its highest activity at 85 °C (Kadziola et al. 2005).

When thermostability of Pcal_1127 was examined by incubating the protein at 90 °C, the optimal growth temperature of *P. calidifontis*, for various intervals of time and measuring the residual activity, Pcal_1127 was found to be highly thermostable with no significant loss in activity even after an incubation of 240 min. As Pcal_1127 was highly stable at 90 °C; therefore, we heated the enzyme at 95 and 100 °C for various intervals of time and examined the residual activity. Half-life of the enzyme was 50 and 15 min at these temperatures, respectively (Fig. 4c). No reports on thermostability of RPPKs are available in literature except for RPPK from *T. kodakarensis* which exhibited

Table 1 Purification of recombinant Pcal_1127

Purification step	Total protein (mg)	Total activity (U)	Specific activity (U/mg)	Purification-fold	Yield (%)
Cell lysate	8.28	869	105	1	100
Heat treatment	2.12	604	285	2.7	69
HiTrap Q	0.43	171	400	3.8	20
Resource Q	0.31	147	480	4.6	17
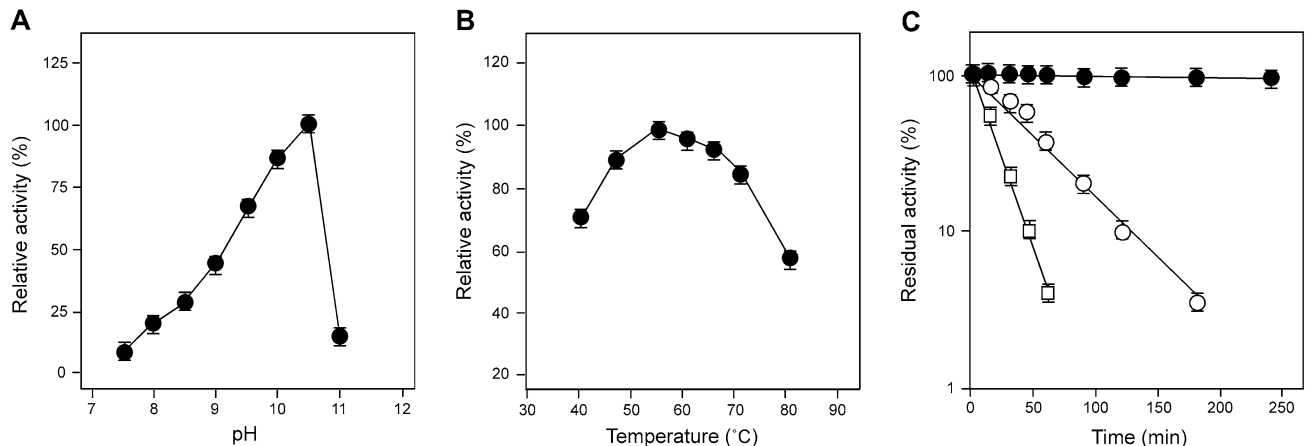
Fig. 4 Effect of pH and temperature on Pcal_1127 enzyme activity. **a** Effect of pH. Activity assays were performed in 50 mM Britton–Robinson buffer at 55 °C. **b** Optimal temperature for enzyme activity. The activity assays were conducted at various temperatures (40–80 °C) in 50 mM Britton–Robinson buffer of pH 10.5. **c** Thermostability of Pcal_1127. Recombinant Pcal_1127, in 20 mM Tris–HCl, was heated at 90 °C (*filled circle*), 95 °C (*open circle*), or in the boiling water (*open square*) for various intervals of time and the residual activity was examined at 55 °C and pH 10.5 in 50 mM Britton–Robinson buffer. The data are average values of three independent experiments

a half-life of 40 min at 70 °C (Rashid et al. 1997). Based on these facts, we propose that Pcal_1127 is the most thermostable RPPK characterized till now. Structural stability of Pcal_1127 was also confirmed by circular dichroism spectroscopy (Fig. 5).

Stability of Pcal_1127 was also examined in the presence of denaturants, such as urea and guanidinium chloride. The protein samples, after treatment with these denaturants for 30 min, were examined for enzyme activity. When Pcal_1127 was incubated in the presence of various concentrations of urea, there was no significant difference in the enzyme activity till 8 M, indicating that there was no inactivation of the protein. Similarly, when guanidinium chloride was used, we found that there was no significant difference in the enzyme activity till 4 M. However, the enzyme activity started decreasing above 4 M final concentration of this denaturant and a 50 % residual activity was detected at 6 M guanidinium chloride.

Pcal_1127 displayed enzyme activity without addition of any metal ion. However, a drastic decrease in enzyme activity was observed when 1 mM EDTA was added in
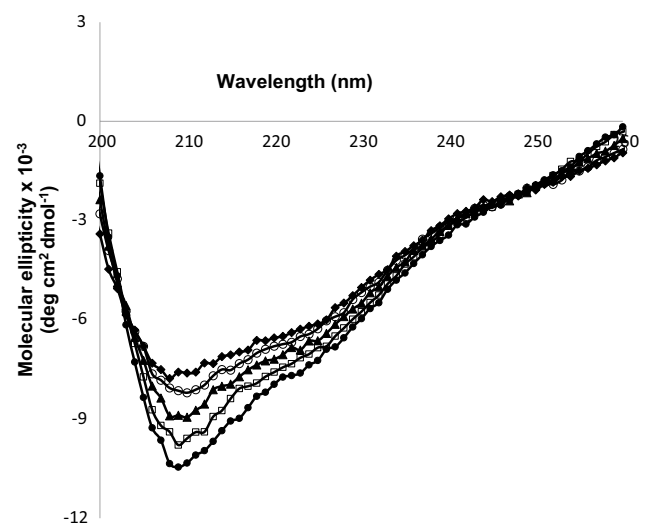

Fig. 5 Circular dichroism studies on Pcal_1127. Far-UV spectrum of Pcal_1127 (200 µg/mL) was analyzed by examining the circular dichroism spectra from 200 to 260 nm at 50 °C (*filled circle*), 60 °C (*open square*), 70 °C (*filled triangle*), 80 °C (*open circle*), and 90 °C (*filled diamond*)
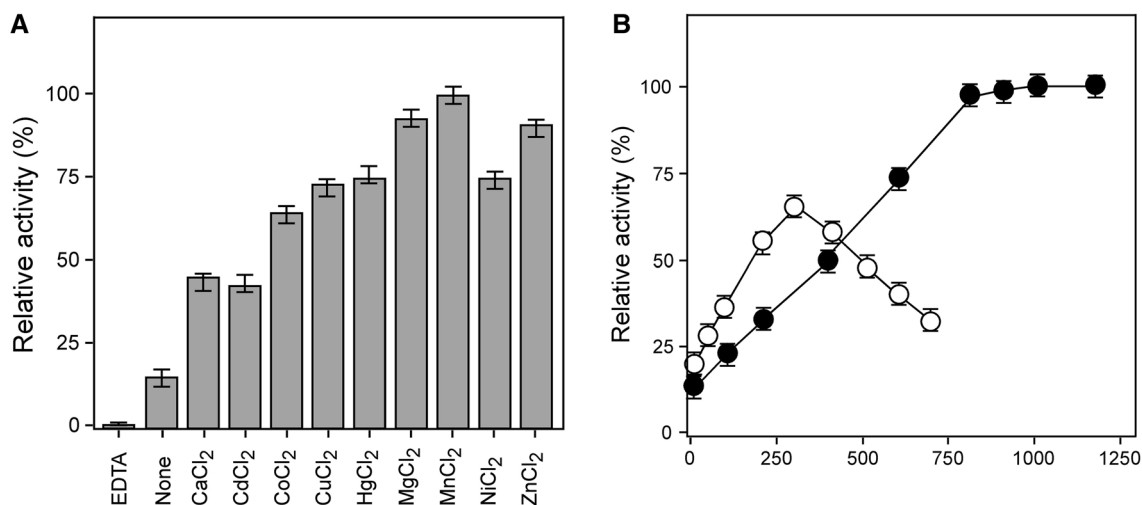
Fig. 6 Effect of various metal ions on the enzyme activity of Pcal_1127. **a** Enzyme activity in the presence of 100 μM chloride salt of each metal. **b** A comparison of enzyme activity in the presence of various concentrations of Mg^{2+} and Mn^{2+}

the reaction mixture. This result indicated that enzyme activity of Pcal_1127 is metal ion dependent. The activity observed without the addition of any metal ion could be attributed to the metal ions bound to the enzyme during production in *E. coli*. Addition of various metal ions in the assay mixture at a final concentration of 100 μM resulted in an increase in enzyme activity to a variable amount (Fig. 6a). Although various metal ions could activate Pcal_1127, highest activity was found in the presence of Mn^{2+} or Mg^{2+}. Therefore, enzyme activity was examined in the presence of various concentrations of Mn^{2+} and highest activity (a 5-fold increase compared with the activity without the addition of any metal ion) was observed at a concentration of 300 μM. There was no increase in the activity at higher concentrations of Mn^{2+}. Similarly, when enzyme activity was examined in the presence of various concentrations of Mg^{2+}, highest activity (an 8-fold increase compared with the activity without the addition of any metal ion) was found at a final concentration of 1 mM (Fig. 6b). Activation of Pcal_1127 by Mg^{2+} or Mn^{2+} is similar to most of the RPPKs from archaeal sources except for the enzyme from *T. kodakarensis* which shows highest activity in the presence of Co^{2+} followed by Ni^{2+} (Rashid et al. 1997).

When pyrophosphate donor specificity of Pcal_1127 was examined, we found that the enzyme could utilize all the four ribonucleoside triphosphates with a marked preference for ATP. In the absence of phosphate ions, highest activity was observed with dATP, a 2-fold higher than that with ATP. However, in the presence of phosphate ions, equivalent amount of activity was observed with dATP and ATP (Fig. 7). Phosphate although activates Pcal_1127 but is not an absolute requirement for the activity of the
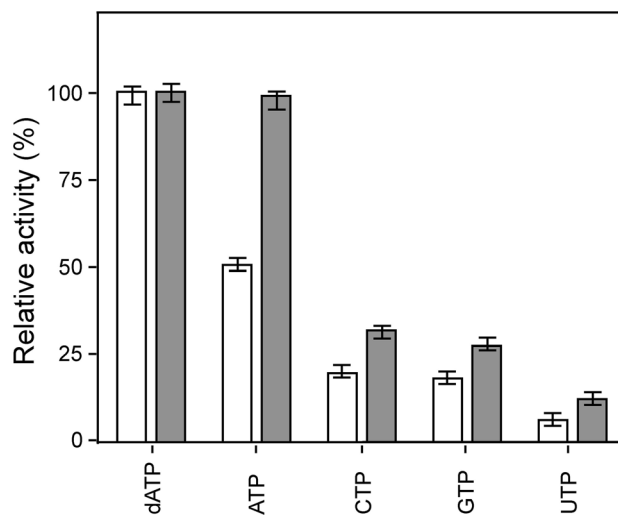

Fig. 7 Substrate specificity of Pcal_1127 in the presence (*filled bars*) and absence (*blank bars*) of phosphate ions. Each substrate was used at a final concentration of 1 mM

enzyme. Apart from phosphate ions, the presence of bovine serum albumin, β-mercaptoethanol, and EDTA at lower concentrations (less than 1 mM) enhanced the enzyme activity of Pcal_1127. A combination of these additives resulted in a 4.5-fold increase in enzyme activity. Similar results have been reported for RPPK from rat liver (Roth et al. 1974).

Similar to other RPPKs (Kadziola et al. 2005; Gibson et al. 1982), the enzyme activity of Pcal_1127 was inhibited by ADP. A 40 % decrease in enzyme activity was observed when ATP and ADP were present in the reaction mixture at an equimolar (1 mM) concentration.

Table 2 Comparison of kinetic parameters of RPPKs from various sources

Source	K_m (μM)		Specific activity (μmol min^{-1} mg^{-1})	References
	R5P	ATP		
P. calidifontis	60	80	480	This work
M. jannaschii	2800	2600	270	Kadziola et al. (2005)
S. solfataricus	ND	ND	67	Andersen et al. (2015)
T. kodakarensis	ND	ND	182	Rashid et al. (1997)
B. subtilis	480	660	190	Arnvig et al. (1990)
B. amyloliquefacien	105	50	37	Zakataeva et al. (2012)
B. caldolyticus	530	310	400	Hove-Jensen and McGuire (2004)
M. tuberculosis	14	25	1.16	Breda et al. (2012)
S. typhimurium	290	193	130	Switzer and Gibson (1978)
E. coli	203	113	170	Willemoës and Hove-Jensen (1997)
Spinach	110	170	13.1	Krath and Hove-Jensen (2001a)
Human	52	21	25	Nosal et al. (1993)
Rubber tree	40	200	12.2	Gallois et al. (1997)

ND no data available

Kinetic parameters

Kinetic parameters towards R-5P were measured by varying the concentration of R-5P and keeping ATP constant at 1 mM. Similarly, when these parameters were measured towards ATP, then R-5P concentration was kept constant at 1 mM and ATP concentration was varied. The enzyme followed the Michaelis–Menton equation. Pcal_1127 exhibited a K_m value of 60 ± 2 μM towards R-5P and 80 ± 3 μM towards ATP. A V_{max} value of 570 μmol min^{-1} mg^{-1} was calculated from Lineweaver–Burk plot. From the V_{max} (570 μmol min^{-1} mg^{-1}) and molecular weight (32,741 Da) of Pcal_1127, a k_{cat} value of 311 s^{-1} was calculated. A comparison of specific activities and K_m values of the characterized RPPK is given in Table 2. Pcal_1127 displayed the highest specific activity among all the characterized RPPKs and a very low K_m value. These features make Pcal_1127 a highly efficient enzyme. Catalytic efficiency (k_{cat}/K_m) of Pcal_1127 was found to be 5183 mM^{-1} s^{-1}. To the best of our knowledge, this is the highest catalytic efficiency of any RPPK characterized till now.

Discussion

Complete genomes of more than 4200 organisms, including 328 eukaryotes, 3650 bacteria, and 223 archaea, have been sequenced (http://www.genome.jp/kegg/catalog/org_list.html). The sequence information has tremendous contribution in identifying the presence or absence of particular genes or metabolic pathway in a particular organism (Fraser et al. 2000; Nelson et al. 2000; Rashid et al. 2002). When we searched the genome sequence of *P. calidifontis* for candidate gene encoding RPPK, we found an open reading frame, Pcal_1127, annotated as ribose-5-phosphate pyrophosphokinase. To examine the properties of Pcal_1127, the gene was expressed in *E. coli* and the gene product was purified. Although Pcal_1127 originates from a hyperthermophile with optimal growth temperature between 90 and 95 °C (Amo et al. 2002), the optimal temperature for the enzyme activity was found 55 °C. This prompted us to examine the thermostability of the enzyme. When we heated the enzyme at 90 °C, the optimal growth temperature of *P. calidifontis*, for various intervals of time and measured the residual activity, no significant loss of enzyme activity could be observed even after an incubation of 240 min. We, therefore, heated the protein in the boiling water, where it displayed a half-life of 15 min. Low optimal temperature (55 °C) for enzyme activity may be attributed to the instability of the substrate at high temperature. Amino acid composition is considered very relevant in thermostability, as it is related to the hydrophobic interactions (Baldwin 2007; Pace 2009). A comparison of amino-acid composition showed that Pcal_1127 has quite high number of hydrophobic residues L and V which constitute 24.6 % of the protein. Furthermore, there are 34 (11.4 %) alanine residues, the best α-helix former, which may be one of the factors responsible for the thermostability of Pcal_1127. Amino-acid content of thermolabile amino acids, such as C, M, Q (each 1.3 %), and N (2.4 %) was very low. These amino acids tend to be avoided in thermostable enzymes (Hensel 1993; Muir et al. 1995; Russell and

Taylor 1995; Russell et al. 1997). High thermostability of Pcal_1127 may be attributed to higher content of α-helix formers along with higher number of hydrophobic residues and lower number of thermolabile amino acids. Recombinant Pcal_1127 exhibited several unique and novel features which include high thermostability, high enzyme activity, and catalytic efficiency. Another unique feature of Pcal_1127 was its highest activity with dATP in the absence of phosphate.

Mostly, the proteins lose their enzyme activities in the presence of high concentrations of denaturants like urea or guanidinium chloride, because these chaotropic agents disturb the native physiological active structure. However, a few proteins from hyperthermophilic archaea are reported to maintain their structures, and hence, the enzyme activities, in the presence of these denaturants (Rasool et al. 2010; Chohan and Rashid 2013; Gharib et al. 2016). We found that there was no inactivation of Pcal_1127 in the presence of even 8 M urea. However, there was a 50 % decrease in activity in the presence of 6 M guanidinium chloride. This can be due to the fact that guanidinium chloride is a salt as well as a denaturant, whereas urea is an uncharged molecule, hence, deficient in ionic strength effects. We could not compare the CD spectra of the protein samples containing urea or guanidium chloride or none due to interference of these chaotropic agents. Structural changes caused by these chaotropic agents are usually studied by recording the fluorescence of the tryptophan residues of the protein samples. Unfortunately, there was no tryptophan residue in the sequence of Pcal_1127; therefore, we could not measure these structural changes, if any.

In conclusion, the results obtained in this study demonstrate that Pcal_1127 exhibits a combination of properties of class I and II RPPKs and is highly stable against temperature and denaturants. Furthermore, the catalytic efficiency reflects that Pcal_1127 is the most efficient RPPK characterized to date.

References

Amo T, Paje ML, Inagaki A, Ezaki S, Atomi H, Imanaka T (2002) *Pyrobaculum calidifontis* sp. nov., a novel hyperthermophilic archaeon that grows in atmospheric air. Archaea 1:113–121

Andersen RW, Leggio LL, Hove-Jensen B, Kadziola A (2015) Structure of dimeric, recombinant *Sulfolobus solfataricus* phosphoribosyl diphosphate synthase: a bent dimer defining the adenine specificity of the substrate ATP. Extremophiles 19:407–415

Arnvig K, Hove-Jensen B, Switzer RL (1990) Purification and properties of phosphoribosyl-diphosphate synthetase from *Bacillus subtilis*. Eur J Biochem 192:195–200

Baldwin RL (2007) Energetics of protein folding. J Mol Biol 371:283–301

Bradford M (1976) A rapid and sensitive method for the quantitation of microgram quantities of protein utilizing the principle of protein dye binding. Anal Biochem 72:248–254

Breda A, Martinelli LKB, Bizarro CV, Rosado LA, Borges CB, Santos DS, Basso LA (2012) Wild-Type phosphoribosylpyrophosphate synthase (PRS) from *Mycobacterium tuberculosis*: a bacterial class II PRS? PLoS One 7:e39245

Cherney MM, Cherney LT, Garen CR, James MN (2011) The structures of *Thermoplasma volcanium* phosphoribosyl pyrophosphate synthetase bound to ribose-5-phosphate and ATP analogs. J Mol Biol 413:844–856

Chohan SM, Rashid N (2013) TK1656, a thermostable L-asparaginase from *Thermococcus kodakaraensis*, exhibiting highest ever reported enzyme activity. J Biosci Bioeng 116:438–443

Eriksen TA, Kadziola A, Bentsen AK, Harlow KW, Larsen S (2000) Structural basis for the function of *Bacillus subtilis* phosphoribosylpyrophosphate synthetase. Nat Struct Biol 7:303–308

Fraser CM, Eisen JA, Salzberg SL (2000) Microbial genome sequencing. Nature 406:799–803

Gallois R, Prevot JC, Clément A, Jacob JL (1997) Purification and characterization of phosphoribosylpyrophosphate synthetase from rubber tree latex. Plant Physiol 115:847–852

Gharib G, Rashid N, Bashir Q, Gardner QA, Akhtar M, Imanaka T (2016) Pcal_1699, an extremely thermostable malate dehydrogenase from hyperthermophilic archaeon *Pyrobaculum calidifontis*. Extremophiles 20:57–67

Gibson KJ, Schuber KR, Switzer RL (1982) Binding of the substrates and the allosteric inhibitor adenosine 5′-diphosphate to phosphoribosylpyrophosphate synthetase from *Salmonella typhimurium*. J Biol Chem 257:2391–2396

Hensel R (1993) Proteins of extreme thermophiles. In: Kates M, Kushner DJ, Matheson AT (eds) The biochemistry of the archaea. Elsevier, Amsterdam, pp 209–221

Hong S, Zhou D, Chen C, Wang W, Lv Y, Ye Y, Zou P, Yv J, Chang X, Yv X, Shi L, Ma Lei (2013) Ribose-phosphate pyrophosphokinase 1 (PRPS1) associated with deltamethrin resistance in *Culex pipiens pallens*. Parasitol Res 112:847–854

Hove-Jensen B (1988) Mutation in the phosphoribosylpyrophosphate synthetase gene (prs) that results in simultaneous requirements for purine and pyrimidine nucleosides, nicotinamide nucleotide, histidine, and tryptophan in *Escherichia coli*. J Bacteriol 170:1148–1152

Hove-Jensen B (2004) Heterooligomeric phosphoribosyl diphosphate synthase of *Saccharomyces cerevisiae*: combinatorial expression of the five PRS genes in *Escherichia coli*. J Biol Chem 279:40345–40350

Hove-Jensen B, McGuire JN (2004) Surface exposed amino acid differences between mesophilic and thermophilic phosphoribosyl diphosphate synthase. Eur J Biochem 271:4526–4533

Jiménez A, Santos MA, Revuelta JL (2008) Phosphoribosyl pyrophosphate synthetase activity affects growth and riboflavin production in *Ashbya gossypii*. BMC Biotechnol 8:67

Kadziola A, Jepsen CH, Johansson E, McGuire J, Larsen S, Hove-Jensen B (2005) Novel class III phosphoribosyl diphosphate synthase: structure and properties of the tetrameric, phosphate-activated, non-allosterically inhibited enzyme from *Methanocaldococcus jannaschii*. J Mol Biol 354:815–828

Kita K, Otsuki T, Ishizuka T, Tatibana M (1989) Rat liver phosphoribosyl pyrophosphate synthetase: existence of the purified enzyme as heterogeneous aggregates and identification of the catalytic subunit. J Biochem 105:736–741

Krath BN, Hove-Jensen B (2001a) Class II recombinant phosphoribosyl diphosphate synthase from spinach. Phosphate independence and diphosphoryl donor specificity. J Biol Chem 276:17851–17856

Krath BN, Hove-Jensen B (2001b) Implications of secondary structure prediction and amino acid sequence comparison of class I and class II phosphoribosyl diphosphate synthases on catalysis, regulation, and quaternary structure. Protein Sci 10:2317–2324

Krath BN, Eriksen TA, Poulsen TS, Hove-Jensen B (1999) Cloning and sequencing of cDNAs specifying a novel class of phospho-ribosyl diphosphate synthase in *Arabidopsis thaliana*. Biochim Biophys Acta 1430:403–408

Li S, Lu T, Peng B, Ding J (2007) Crystal structure of human phos-phoribosylpyrophosphate synthetase 1 reveals a novel allosteric site. Biochem J 401:39–47

Lucarelli AP, Buroni S, Pasca MR, Rizzi M, Cavagnino A, Valentini G, Riccardi G, Chiarelli LR (2010) *Mycobacterium tuberculosis* phosphoribosylpyrophosphate synthetase: biochemical features of a crucial enzyme for mycobacterial cell wall biosynthesis. PLoS One 5:e15494

Muir JM, Russell RJM, Hough DW, Danson MJ (1995) Citrate syn-thase from the hyperthermophilic archaeon *Pyrococcus furiosus*. Protein Eng 8:583–592

Nelson KE, Paulsen IT, Heidelberg JF, Fraser CM (2000) Status of genome projects for nonpathogenic bacteria and archaea. Nat Biotechnol 18:1049–1054

Nosal JM, Switzer RL, Becker MA (1993) Overexpression, purifica-tion, and characterization of recombinant human 5-phosphoribo-syl-1-pyrophosphate synthetase isozymes I and II. J Biol Chem 268:10168–10175

Pace CN (2009) Energetics of protein hydrogen bonds. Nat Struct Mol Biol 16:681–682

Rashid N, Morikawa M, Imanaka T (1997) Gene Cloning and Char-acterization of recombinant ribose phosphate pyrophosphokinase from a hyperthermophilic archaeon. J Biosci Bioeng 83:412–418

Rashid N, Imanaka H, Kanai T, Fukui T, Atomi H, Imanaka T (2002) A novel candidate for the true fructose-1,6-bisphosphatase in archaea. J Biol Chem 277:30649–30655

Rasool N, Rashid N, Iftikhar S, Akhtar M (2010) N-terminal deletion of Tk1689, a subtilisin-like serine protease from *Thermococcus kodakaraensis*, copes with its cytotoxicity in *Escherichia coli*. J Biosci Bioeng 110:381–385

Roth DG, Shelton E, Deuel TF (1974) Purification and properties of phosphoribosyl pyrophosphate synthetase from rat liver. J Biol Chem 249:291–296

Russell RJM, Ferguson JMC, Haugh DW, Danson MJ, Taylor GL (1997) The crystal structure of citrate synthase from the hyper-thermophilic archaeon *Pyrococcus furiosus* at 1.9 Å resolution. Biochemistry 36:9983–9994

Russell RJM, Taylor GL (1995) Engineering thermostability: lessons from thermophilic proteins. Curr Opin Biotechnol 6:370–374

Switzer RL (1969) Regulation and mechanism of phosphoribo-sylpyrophosphate synthetase I. purification and properties of the enzyme from *Salmonella typhimurium*. J Biol Chem 244:2854–2863

Switzer RL, Gibson KJ (1978) Phosphoribosylpyrophosphate syn-thetase (ribose-5-phosphate pyrophosphokinase) from *Salmo-nella typhimurium*. Methods Enzymol 51:3–11

Willemoës M, Hove-Jensen B (1997) Binding of divalent magnesium by *Escherichia coli* phosphoribosyl diphosphate synthetase. Bio-chemistry 36:5078–5083

Willemoës M, Hove-Jensen B, Larsen S (2000) Steady state kinetic model for the binding of substrates and allosteric effectors to *Escherichia coli* phosphoribosyl-diphosphate synthase. J Biol Chem 275:35408–35412

Zakataeva NP, Romanenkov DV, Skripnikova VS, Vitushkina MV, Livshits VA, Kivero AD, Novikova AE (2012) Wild-type and feedback-resistant phosphoribosyl pyrophosphate synthetases from *Bacillus amyloliquefaciens*: purification, characterization, and application to increase purine nucleoside production. Appl Microbiol Biotechnol 93:2023–2033